Reconstructing Cardiac Shape via Constrained Voronoi Diagram and Cyclic Dynamic Time Wrapping From CMR

Min Wan[1], Yuli Yang[1], Xiaodan Zhao[2], Shuang Leng[2], Jun-Mei Zhang[2,3], Ru San Tan[2,3], Liang Zhong[2,3]

Abstract

Reconstructing cardiac shapes from CMR short axis parallel contours is a prerequisite task for downstreaming analysis and diagnosis. This task, however, is not trivial when the inflow and outflow tract must be taken into account. These tracts are a difficulty for reconstructing whole cardiac shapes from CMR. We aimed to develop a method to reconstruct either left cardiac structure or right cardiac structure with minimal user assistance in a unified geometric framework. Ventricular, atrial, and arteries contours were delineated on short axis images. Cyclic dynamic time wrapping (DTW) method were utilized to triangulate two parallel contours on neighboring imaging slices. Reconstructing three contours on inflow and outflow tracts were divided into two parts. The outer part was reconstructed from the lower contour and the convex hull of two upper contours. The interior part was parobolic surfaces fit to points not existing in the convex hull and the Voronoi cell centroids. All cases were automatically reconstructed successfully with average computational time less than one minute. Reconstructed shape have anatomically reasonable structures.

1. Introduction

Because of its intrisic blood-to-tissue contrast and high reproducibility, cardiac magnetic resonance (CMR) imaging has been considered the non-invasive gold standard for evaluating cardiac function [1, 2]. Reconstructing cardiac shapes from CMR is then a prerequisite task for quantitative analysis and diagnosis.

Extensive studies have focus on the left ventricle (LV) modelling from contours. From early approaches [3] using idealized ellipsoidal shapes to approaches [4, 5] using more sophisticated superquadric shapes, triangulating two parallel contours is a basic operation. However, these reconstructed models have not included all information from CMR images. Only contours from the basal slice to the apex slice were used. Two anatomic parts in left cardiac structure, i.e., the atrioventricular junction (LV inflow tract) and the aorto-ventricular junction (LV outflow tract), as well as part of left atrium (LA) and aorta (AO), were not reconstructed into the result. Some recent approaches [6–9] used a population-based (statistical) model and fit each patient's images to it. Adapting the statistical model to a patient-specific model involved certain heuristic methods. The precision of the patient-specific model was limited. Meanwhile, few attentions were drawn to the right ventricle (RV) reconstruction due to its complex shape and high inter individual variability.

Our relevant work [10, 11] addressed reconstruction of left and right cardiac strucutre from a variational point of view, respectively. The methods optimized a variational energy functional compromising the closeness between the reconstructed surface and point clouds and the smoothness. The reconstructed surface on the inflow and outflow junction were the result of the smoothness term. A large smoothness term, however, could possibly make the original detail on the surfaces underlooked. Besides, due to the complex crescent shape of right ventricle (RV), extra operations were included in right cardiac modeling. The demand of a unified reconstruction tool with more geometrical precision motivates this study.

In this study, we proposed a novel method to reconstruct cardiac shapes from short axis contours, which works on both left and right cardiac structures. Cine MR images were acquired and all ventricular, atrial, aortic and pulmonary artery contours were delineated on short axis images. Surfaces between two parallel contours were triangulated via cyclic DTW algorithm [12]. Reconstruction between three contours were divide into two parts. Firstly the convex hull of upper two contours, e.g., arota and atrium, were connected to lower ventricular contour. This triangulated result constitutes the outer part of the inflow/outflow tracts. Secondly the interior points not existing in the convex hull were utilized to generate a parabolic surface forming the interior part. Voronoi cell centroids in the Voronoi diagram constrained to the lower contour were utilized as the apex of interior parabolic surface.

2. Methods

The method proposed in this paper includes two stages: (1) contour delineation; (2) triangulation between parallel contours. The second stage reconstructs a triangulated sur-

 ISSN: 2325-887X DOI: 10.22489/CinC.2019.190

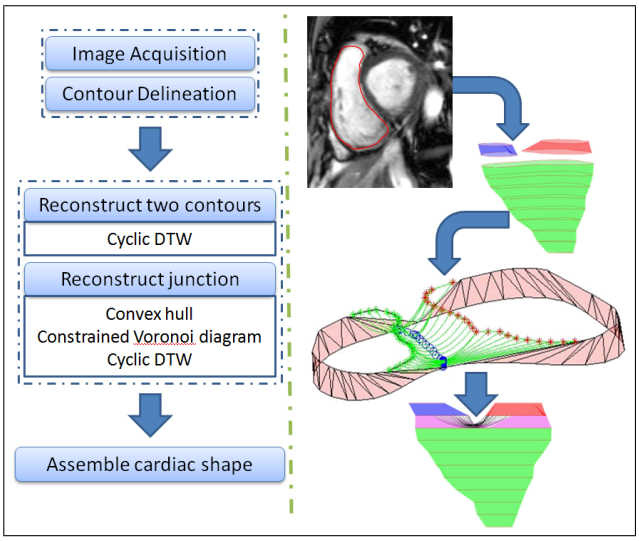

Figure 1. Flowchart of the proposed method. Several alternative implementations are provided for each stage. The implementations we ultilized are underlined.

face mesh between contours on multiple parallel imaging slices. The flowchart of the method is shown in Figure 1.

Triangulating two parallel contours on neiboring imaging slices, i.e., one upper contour and one lower contour, has been studied extensively. However, triangulating multiple contours, such as two upper contours and one lower contour, is not trivial. Reconstructing the whole cardiac shape will confront such challenges on left/right ventricle inflow and outflow tracts. More specifically, determine the connectness among two upper contours representing LA and AO, and one lower LV contour, or RA, PA, and RV, is a significant yet challenging task.

In this section, we formulate both the trivial and difficult triangulation problem into a unified framework based on cyclic DTW. All stages of the method will be described in detail, especially the challenging task of triangulating RA, PA and RV contours. Considering the complex crescent shape in RV and its intrinsic difficulty, we use right cardiac structure (RV, RA, PA) for discussion without loss of generality.

2.1. Contour Delineation

RV endocardial boundary as well as those of RA and PA were delineated by trained experts using CMRtools (Cardiovascular Solution, UK). Contours were drawn in a consistent counterclockwise direction throughout all slices. Contours from all parallel imaging slices were transformed into the patient-based coordinate system according to the imaging specification, e.g., the pixel spacing, the image position, and the image orientation. These image specification are contained in the DICOM file meta information, and the transformation from 2D planar borders to 3D point clouds is as follows.

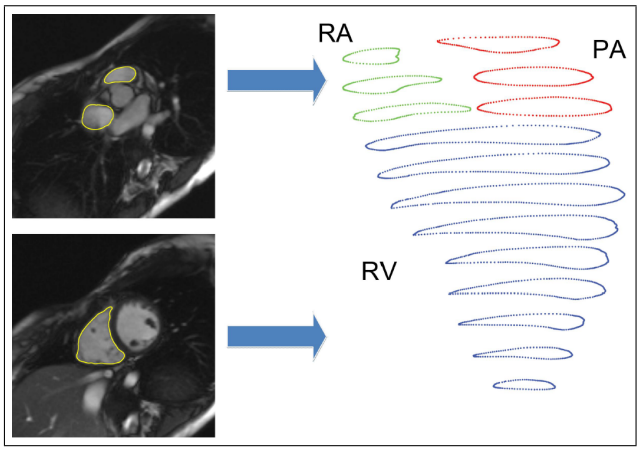

Figure 2. Contours transformation

$$\begin{bmatrix} x \\ y \\ z \\ 1 \end{bmatrix} = \begin{bmatrix} U_x\triangle u & V_x\triangle v & 0 & P_x \\ U_y\triangle u & V_y\triangle v & 0 & P_y \\ U_z\triangle u & V_z\triangle v & 0 & P_z \\ 0 & 0 & 0 & 1 \end{bmatrix} \begin{bmatrix} u \\ v \\ 0 \\ 1 \end{bmatrix}, \quad (1)$$

where (u, v) is the 2D coordinate, (x, y, z) is the transformed 3D coordinate, (P_x, P_y, P_z) is the image position (cf. DICOM attribute (0020,0032)), $(U_{x,y,z}, V_{x,y,z})$ is the image orientation (cf. DICOM attribute (0020,0037)), and $(\triangle u, \triangle v)$ is the pixel spacing (cf. DICOM attribute (0028,0030)).

2.2. Triangulation between Two Contours

$DTW(A, B)$ between two series is defined as the cost of the optimal alignment between A and B, i.e., $DTW(A, B) = d'(m-1, n-1)$, where

$$d'(i,j) = \begin{cases} \delta(a_0, b_0), \text{ if } i = j = 0 \\ d(i-1, 0) + \delta(a_i, b_0), \text{ if } i > 0 \text{ and } j = 0 \\ d'(0, j-1) + \delta(a_0, b_j), \text{ if } i = 0 \text{ and } j > 0 \\ \min \left\{ \begin{matrix} d'(i-1, j-1) \\ d'(i-1, j), \\ d'(i, j-1) \end{matrix} \right\} + \delta(a_i, b_j) \end{cases}$$

$\delta(\cdot, \cdot)$ is the distance between two elements from A and B, usually the Euclidean distance in geometry applications. Cyclic DTW is defined to measure dissimilarity between two closed curves [12]. The minimal DTW between arbitary cyclic shift of A and B is cyclic DTW as follows.

$$CDTW([A], [B]) = \min_{0 \le k < m} \left(\min_{0 \le \ell < n} DTW\left(\sigma^k(A), \sigma^\ell(B)\right) \right),$$

where $\sigma^k(A)$, $\sigma^\ell(B)$ are cyclic k-shift of A and cyclic ℓ-shift of B. The optimized alignment between A and B de-

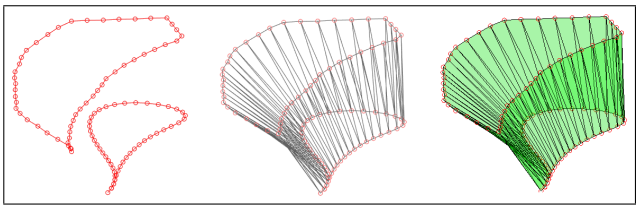

Figure 3. Left: two RV contours; Middle: alignment via cyclic DTW; Right: Triangulated surface

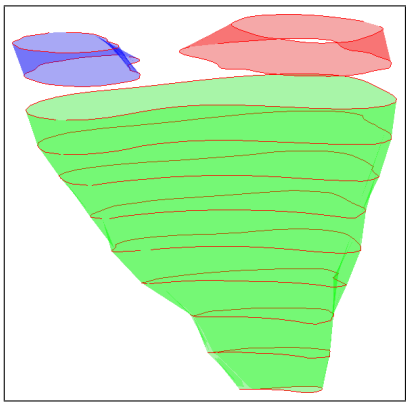

Figure 4. A right cardiac surface without inflow/outflow tracts

fines the connection between points and the triangulation as illustrated in Figure 3.

Using cyclic DTW to triangulate RV, RA, and PA, we obtainted a right cardiac surface without the inflow and outflow tract as shown in Figure 4.

2.3. Triangulation between Three Contours

The challenging part is to reconstruct the missing region in Figure 4, equivalently triangulating among three contours, i.e., upper RA, upper PA, and lower RV. To tackle this issue, we proposed the following algorithm, several steps of which were illustrated in Figure 5.

1. Compute convex hull of PA and RA on the upper imaging plane: $ConvHull$.
2. Triangulate $ConvHull$ and RV via cyclic DTW;
3. Find points in PA and RA not existing in $ConvHull$: $RemPA$,$RemRA$;
4. Align $RemPA$ and $RemRA$ via DTW;
5. Find Voronoi cell centroids of the $RemPA$ and $RemRA$ Voronoi diagram constrained to RV: $VDCen$;
6. Fit each tuple of three points $\{a, b, c\}, a \in RemPA, b \in RemRA, c \in VDCen$ to a parabolic curve;
7. Triangulate all parabolic curves consisting of $RemPA$, $RemRA$, and $VDCen$;

The whole reconstructed right cardiac model including RV, RA and PA was shown in Figure 6.

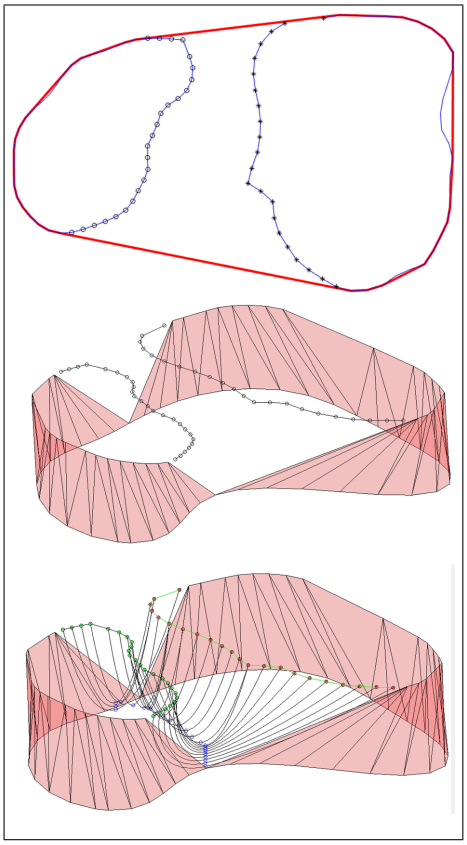

Figure 5. Top: RA, PA in blue and $ConvHull$ in red; Middle: Triangulate $ConvHull$ and RV, $RemPA$,$RemRA$ in black; Down: Triangulate $RemPA$,$RemRA$ and $VDCen$

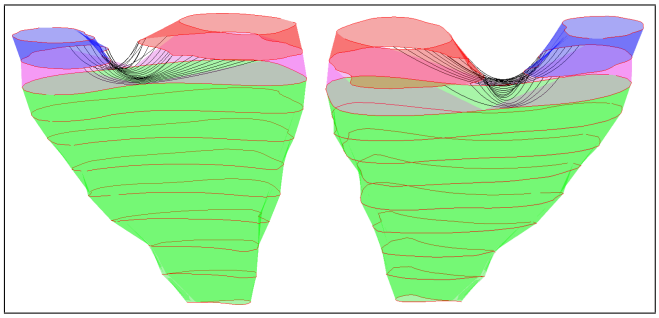

Figure 6. A whole right cardiac surface model from two views

3. Results

The methods were experimented on ten subjects (aged 17-66, 2 males and 8 females). All images were acquired on a 1.5T Siemens MR scanner with ECG gating, including parallel short axis and long axis images. Short axis images were scanned on 12 to 14 imaging slices. Each image slice was acquired in a single breathhold. The imaging parameters were as follows: field of view (FOV) = 320 mm, image size = 192 150, pixel spacing = 1.77 1.77 mm, slice thickness/spacing = 8/8 mm, TR/TE/flip angle = 68/1 ms/70. Short axis image sequences typically had 22 frames per cardiac cycle.

The algorithms were executed on a 2.5GHz CPU desktop. The average computation time was less than one minute. The reconstructed shapes had visually reasonable junction appearance, which validates our proof of concept.

4. Conclusions

In this study, we proposed a method based on cyclic DTW and constrained Voronoi diagram to reconstruct the cardiac shape from short axis contours. By computing cyclic DTW between two contours, two contours could be optimally aligned and well triangulated. To tackle the difficult reconstruction task on the inflow and outflow tracts, we design an algorithm to generate the junction surface consisting of two parts, (a) the outer surface connecting the convex hull of upper two contours and lower single contour; and (b) the interior surface connecting points not existing in the convex hull and the Voronoi cell centroids. The method applies to both left cardiac structure and right cardiac structure with minimal user assistance in a unified geometric framework.

Acknowledgements

This work was supported in part by grants from National Natural Science Foundation of China (NSFC 61562060,61801203),National Medical Research Council Grant (NMRC/EDG/1037/2013; NMRC/OFIRG/0018/2016), Natural Science Foundation of Jiangxi(20171BAB212008) Biomedical Research Council Research Grant (14/1/32/24/002).

References

[1] Sakuma H, Fujita N, Foo T, Caputo GR, Nelson S, Hartiala J, Shimakawa A, Higgins C. Evaluation of left ventricular volume and mass with breath-hold cine mr imaging. Radiology 1993;188(2):377–380.

[2] La Gerche A, Claessen G, Van de Bruaene A, Pattyn N, Van Cleemput J, Gewillig M, Bogaert J, Dymarkowski S, Claus P, Heidbuchel H. Cardiac mri a new gold standard for ventricular volume quantification during high-intensity exercise. Circulation Cardiovascular Imaging 2013;6(2):329–338.

[3] McQueen DM, Peskin CS. A three-dimensional computer model of the human heart for studying cardiac fluid dynamics. ACM SIGGRAPH Computer Graphics 2000;34(1):56–60.

[4] Bardinet E, Cohen LD, Ayache N. Tracking and motion analysis of the left ventricle with deformable superquadrics. Medical image analysis 1996;1(2):129–149.

[5] Metaxas D, Terzopoulos D. Shape and nonrigid motion estimation through physics-based synthesis. Pattern Analysis and Machine Intelligence IEEE Transactions on 1993; 15(6):580–591.

[6] Frangi AF, Rueckert D, Schnabel J, Niessen WJ, et al. Automatic construction of multiple-object three-dimensional statistical shape models: Application to cardiac modeling. Medical Imaging IEEE Transactions on 2002;21(9):1151–1166.

[7] Lötjönen J, Kivistö S, Koikkalainen J, Smutek D, Lauerma K. Statistical shape model of atria, ventricles and epicardium from short-and long-axis mr images. Medical image analysis 2004;8(3):371–386.

[8] Lorenz C, Berg Jv. A comprehensive shape model of the heart. Medical image analysis 2006;10(4):657–670.

[9] Ecabert O, Peters J, Weese J. Modeling shape variability for full heart segmentation in cardiac computed-tomography images. In Medical Imaging. International Society for Optics and Photonics, 2006; 61443R–61443R.

[10] Wan M, Huang W, Zhang JM, Zhao X, San Tan R, Wan X, Zhong L. Variational reconstruction of left cardiac structure from cmr images. PloS one 2015;10(12):e0145570.

[11] Zhong L, Wan M, Su Y, Teo SK, Lim CW, Zhao X, Zhang JM, Su BY, Le Tan J, Tan RS. Graph-cuts based reconstructing patient specific right ventricle: First human study. In Engineering in Medicine and Biology Society (EMBC), 2014 36th Annual International Conference of the IEEE. IEEE, 2014; 6770–6773.

[12] Palazn-Gonzlez V, Marzal A. On the dynamic time warping of cyclic sequences for shape retrieval . Image Vision Computing 2012;30(12):978–990.

Address for correspondence:

Liang Zhong
National Heart Centre Singapore, 5 Hospital Drive, Singapore 169609
zhong.liang@nhcs.com.sg
Min Wan
Nanchang University, Nanchang, Jiangxi, P.R.China 330031
wanmin@ncu.edu.cn